Supplemental Information to Fermi Surface of a System with Strong Valence Fluctuations: Evidence for a Non-Integer Count of Valence Electrons in $EuIr_2Si_2$

K. Götze,[1,2,*] B. Bergk,[1,3] O. Ignatchik,[1] A. Polyakov,[1] I. Kraft,[4,5] V. Lorenz,[6] H. Rosner,[4] T. Förster,[1] S. Seiro,[4,6] I. Sheikin,[7] J. Wosnitza,[1,5] and C. Geibel[4,†]

[1] *Hochfeld-Magnetlabor Dresden (HLD-EMFL) and Würzburg-Dresden Cluster of Excellence ct.qmat, Helmholtz-Zentrum Dresden-Rossendorf, 01328 Dresden, Germany*

[2] *Department of Physics, University of Warwick, Coventry, CV4 7AL, United Kingdom*

[3] *Institut für Werkstoffwissenschaft, TU Dresden, 01062 Dresden, Germany*

[4] *Max Planck Institute for Chemical Physics of Solids, 01187 Dresden, Germany*

[5] *Institut für Festkörper- und Materialphysik, Technische Universität Dresden, 01062 Dresden, Germany*

[6] *Leibniz IFW Dresden, 01069 Dresden, Germany*

[7] *Laboratoire National des Champs Magnétiques Intenses (LNCMI-EMFL), CNRS, UGA, 38042 Grenoble, France*

(Dated: March 24, 2022)

* kathrin.goetze@desy.de; Present address: Deutsches Elektronen-Synchrotron (DESY), 22607 Hamburg, Germany.

† christoph.geibel@cpfs.mpg.de

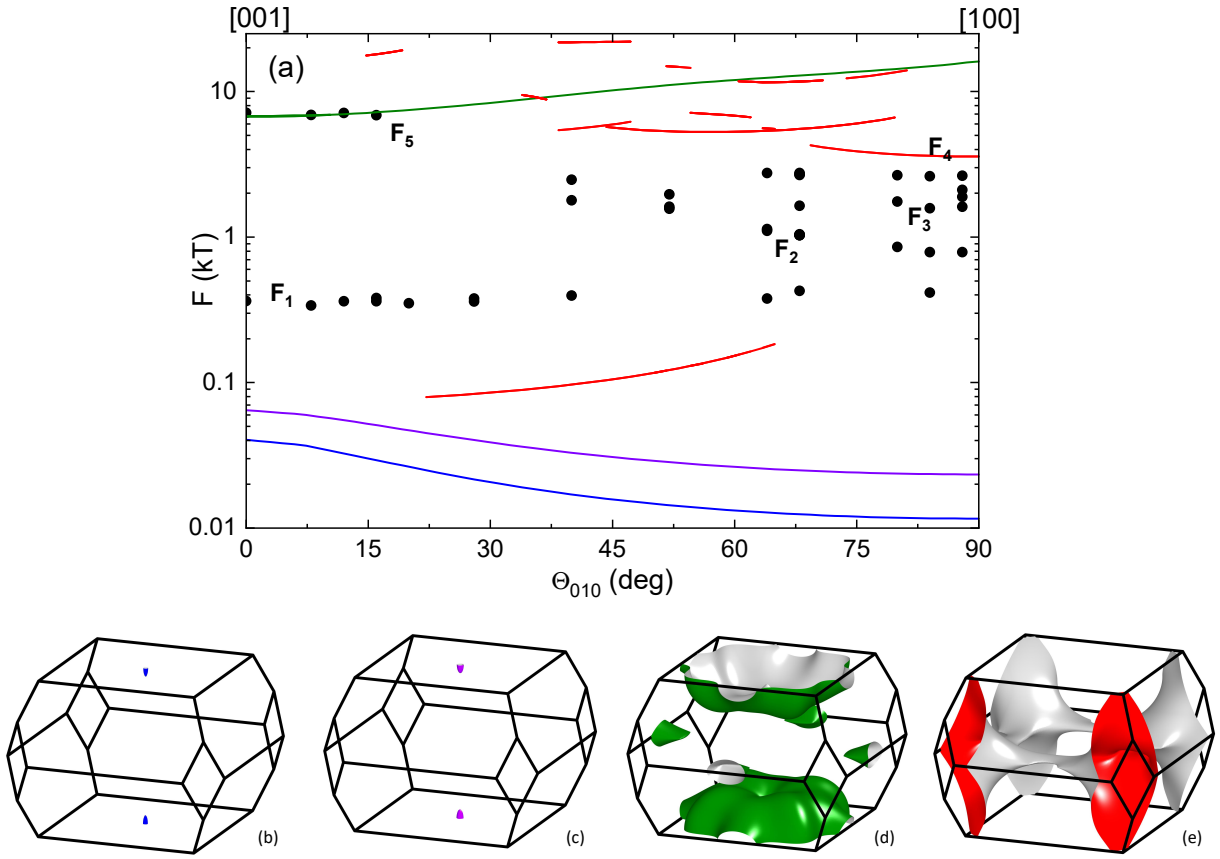

FIG. S1. (a) Comparison of experimental data (black symbols) and calculated frequencies (red, green, blue, and purple lines) obtained from band-structure calculations for divalent europium. Color coding corresponds to the depiction of the calculated FSs from band 46 in (b), band 47 in (c), band 48 in (d), and band 49 in (e)

A. Calculated dHvA frequencies and FSs for divalent Eu

Figure S1(a) shows the quantum-oscillation frequencies derived from the theoretically determined FSs (Figs. S1(b)–(e)) for divalent Eu in $EuIr_2Si_2$. The comparison to our experimental data (black symbols) shows that there is hardly any correspondence. As shown and discussed in the main text, the calculations for $Eu^{2.8+}$ give the best agreement between experiment and calculation.

B. Frequency F_1 and small Fermi surface pockets in calculations based on $Eu^{2.8+}$

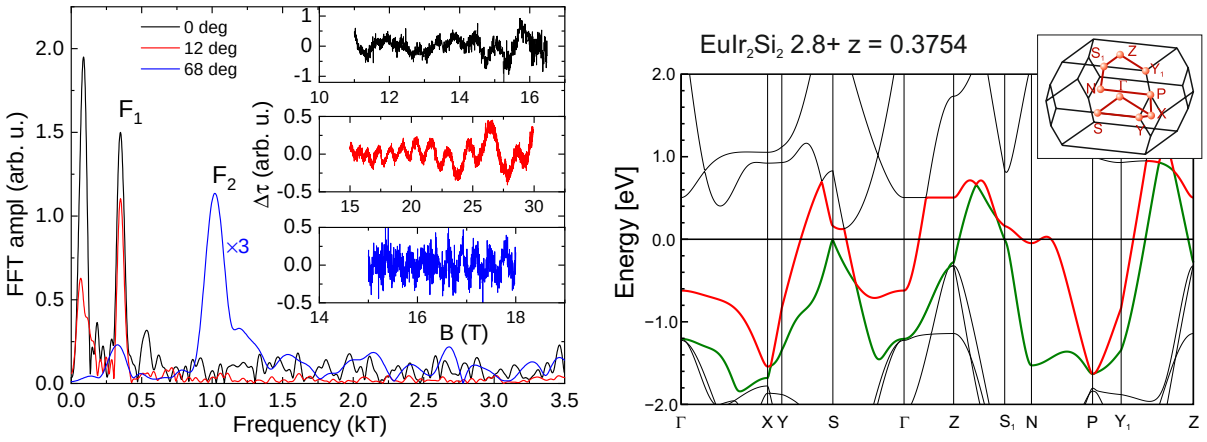

(a) (b)

FIG. S2. (a) Frequency spectrum obtained by FFT of the oscillating part of the torque signal after background subtraction (shown in the insets) for $\Theta_{010} = 0°, 12°, 68°$. (b) Band dispersion along the high-symmetry axes of $EuIr_2Si_2$ for $Eu^{2.8+}$ with $z = 0.3754$. Inset: Brillouin zone and its symmetry points.

In Fig. S2 (a), we show examples of frequency spectra focusing on the low frequency F_1. These data were measured upon rotation from $B\|[001]$ to $B\|[100]$. The black and red curves (measured at 0 and 12°, respectively) both show a clear peak at 350 T. For $\Theta_{010} = 68°$ (blue), the spectrum is dominated by the higher frequency F_2 but nevertheless there is a distinct peak at 330 T. The insets of Fig. S2 (a) show the oscillating part of the data just mentioned.

The band dispersion for $EuIr_2Si_2$ with $Eu^{2.8+}$ is shown in Fig. S2 (b) with band 48 highlighted in green and band 49 in red. Band 49 crosses the Fermi energy within a very small energy range between S1 and N, and between N and P leading to the small FS pockets, shown in Fig. 3(d) of the main text, which are the origin of the quantum oscillations with frequency F_1. The high-symmetry points of the Brillouin zone are annotated in the inset of Fig. S2 (b).

C. Dingle temperature

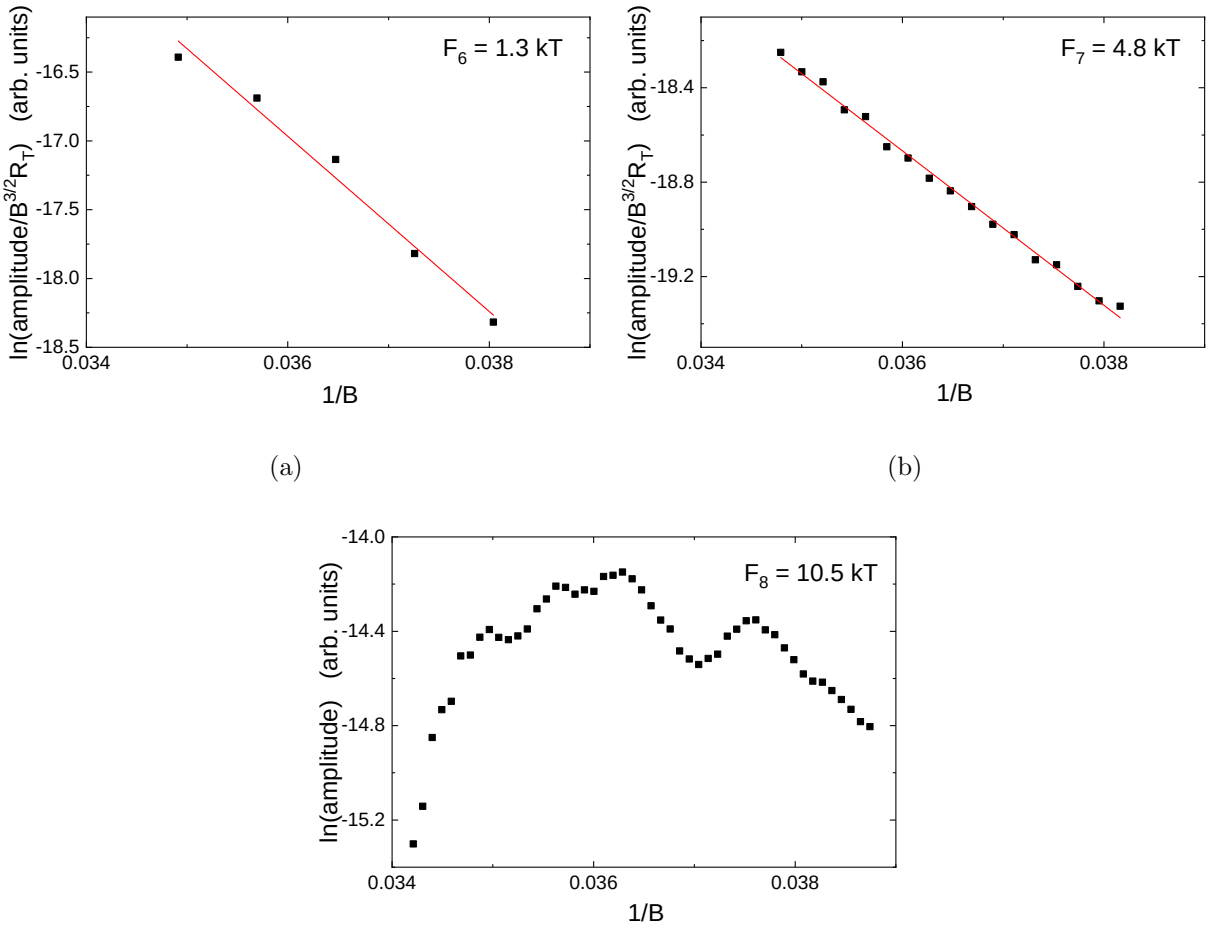

FIG. S3. Inverse field dependence of the FFT amplitudes shown as Dingle plots for frequencies F_6 (a) and F_7 (b) including linear fits, and of the logarithm of the FFT amplitudes for frequency F_8 (c), all at $\Theta_{110} = 84°$ and 70 mK. The Dingle temperatures for F_6 and F_7 are 7.9 K and 3.7 K, respectively. FFTs were performed over four oscillation periods for each data point.

The field dependence of the quantum-oscillation amplitudes measured by the torque technique can be described by

$$A \propto R_T R_D B^{3/2},$$

with amplitude A, temperature damping factor R_T, and Dingle factor R_D [S1]. The Dingle factor $R_D = \exp(-\alpha m_b T_D/B)$ ($\alpha \approx 14.69$ T/K) depends on the band mass m_b and the Dingle temperature which is inversely proportional to the scattering rate τ by $T_D = \hbar/(2\pi k_B \tau)$.

The Dingle temperature is, therefore, a measure for sample quality. So-called Dingle plots as shown in Figs. S3 (a) and S3 (b) for F_6 and F_7 display the amplitude of the dHvA oscillations of a certain frequency as $\ln(A/[R_T B^{3/2}])$ vs $1/B$. The Dingle temperature can then be determined from the slope of a linear fit to the data [S2]. The dHvA amplitudes in the Dingle plots of F_6 and F_7 show the expected linear dependence, while those of F_8 (here shown as the logarithm of the amplitude of the dHvA frequencies) deviate clearly from linearity and decrease strongly for high fields indicating additional scattering mechanisms.

[S1] D. Shoenberg, *Magnetic Oscillations in Metals* (Cambridge University Press, Cambridge, 1984).

[S2] For the determination of the Dingle temperature from the slope of the linear fits we have replaced the band mass m_b by the effective mass m_{eff}, which has been determined from the temperature-dependent decrease of the amplitudes.